CHEMICAL KINETICS IN H_2O AND D_2O UNDER HYDROTHERMAL CONDITIONS

K. Ghandi* [1], C. D. Alcorn [1], G. Legate [1], P. W. Percival*[2] and J.-C. Brodovitch[2]
[1] Mount Allison University, Sackville, New Brunswick, Canada
[2] Simon Fraser University, Burnaby, British Columbia, Canada

Abstract

Muonium (Mu = μ^+e^-) is a light analogue of the H-atom. Studies of Mu chemical kinetics have been extended to supercritical water, a medium in some designs of future generation nuclear reactors. The Supercritical-Water-Cooled Reactor (SCWR) would operate at higher temperatures than current pressurized water-cooled reactors, and the lack of knowledge of water radiolysis under supercritical conditions constitutes a technology gap for SCWR development. Accurate modeling of chemistry in a SCWR requires data on kinetics of reactions involved in the radiolysis of water. In this paper, we first review our measurements of kinetics in H_2O and then describe new data for D_2O under sub- and supercritical conditions.

1. Introduction

The critical point of water is 374°C and 221 bar. Current interest in supercritical water lies mainly in the area of hazardous waste destruction by supercritical water oxidation (see as an example Ref. [1]) and its use as a coolant in fossil-fired supercritical water-cooled plants and its potential use in Supercritical-Water-Cooled Reactors (SCWRs) [2]. In addition to the nuclear power and waste treatment industries, supercritical water is used for materials processing and chemical synthesis (aquathermolysis) [3]. Figure 1 shows the phase diagram of water and the relevant industrial and chemical applications under different temperature and pressure conditions.

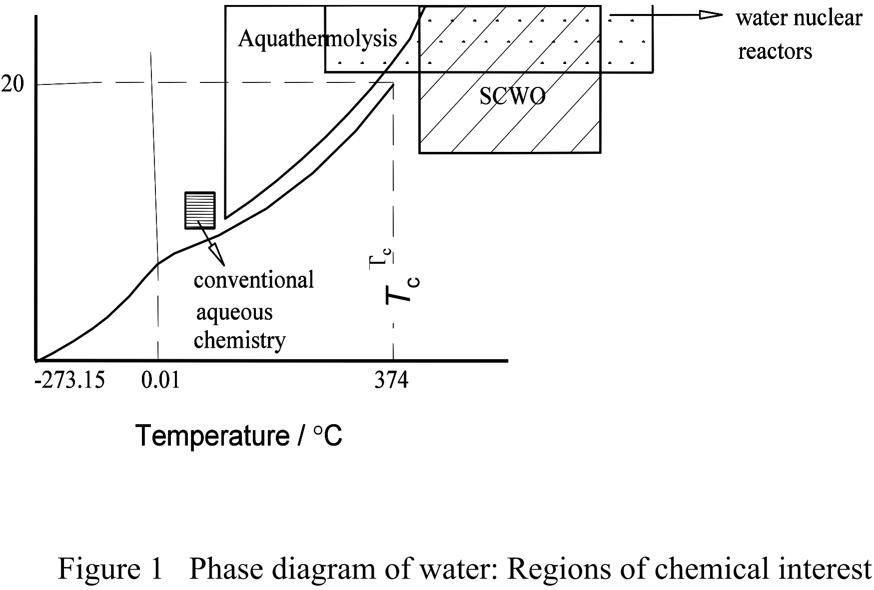

Figure 1 Phase diagram of water: Regions of chemical interest.

Given the significance of industrial chemistry in supercritical water, there is a need to understand the relevant reaction kinetics and their responses to changes in reaction variables. Since it is difficult to measure the kinetics of transient species involved in the radiolysis of water under the extreme conditions of a SCWR, most of the available kinetics data in this region are extrapolated from kinetics data at much lower temperatures [4]. For activation-controlled reactions, the Arrhenius equation (1) is usually used:

$$k_{\mathrm{react}} = Ae^{-E_{\mathrm{a}}/kT} \tag{1}$$

where k_{react} is the activation-controlled rate constant, E_{a} is the activation energy of the reaction, k is the Boltzmann constant, T is the temperature and A is a pre-exponential factor.

For diffusion-controlled reactions, the Smoluchowski equation (2) is widely used [4]:

$$k_{\mathrm{d}} = 4000\pi(D_{\mathrm{A}} + D_{\mathrm{B}})r_{\mathrm{AB}}\, N_{\mathrm{Av}} \tag{2}$$

where k_{d} is the diffusion-controlled rate constant, D_{A} and D_{B} are the diffusion coefficients of the reactants, r_{AB} is the distance at which reactants A and B can react and N_{Av} is Avogadro's number (6.022×10^{-23}).

The kinetics of reactions that are close to diffusion-controlled, and are therefore subject to both diffusion and activation processes, can be modelled by the Noyes equation:

$$1/k_{\mathrm{obs}} = 1/k_{\mathrm{diff}} + 1/k_{\mathrm{react}} \tag{3}$$

where k_{obs} is the observed rate constant. This has been widely employed to predict the rate constants of reactions involved in the radiolysis of water [4]. The accuracy of the predicted rate constants at high temperatures and pressures has, however, been questioned [5].

Clearly, modelling of aqueous chemistry in the heat transport systems of Pressurized Water-cooled Reactors (PWRs), Pressurized Heavy Water Cooled Reactors (PHWRs) and the SCWR requires accurate data on the rate constants of reactions involved in the radiolysis of water and the action of water treatment additives. Unfortunately, most experimental data do not even extend to the temperatures used in current PWRs and PHWRs, typically around 320°C, well short of the supercritical conditions (500–650°C) envisaged in Generation IV designs. Thus, a major technology gap for SCWR development is the lack of knowledge of water radiolysis under supercritical conditions. We have recently initiated a project to explore kinetics in this regime, with an initial focus on the range of 320°C to 450°C.

In this paper we will review briefly what is known about kinetics in supercritical water and compare that with the kinetics in water at lower temperatures. We will describe the experimental methods that we use for our studies, and finally we will present some new data and discuss the implications for SCWRs followed by some conclusions.

2. Kinetics in supercritical water

We first consider the findings of studies of SCW oxidation. Although in general the oxidation rates in supercritical water are substantially higher than subcritical conditions [6], the rate constants depend significantly on density [7]. The problem with kinetic studies of SCW oxidation is that the mechanisms are too complex to allow definitive identification of the fundamental chemical or physical processes responsible for the observed density or temperature dependence. In that sense, studies of radiolysis and even better, elementary reactions would be more useful. Nevertheless, some trends can be learned from studies of SCW oxidation. For example, diffusion coefficients increase significantly with temperature in liquid water or under supercritical conditions, and decrease with density under supercritical conditions. A large increase in the diffusion coefficients of the reaction species has been noted at the critical point and the diffusion rates of water under supercritical conditions found to be approximately 60 times as large as those observed under ambient conditions [7].

The rate constant at the diffusion-controlled limit is often estimated using the Smoluchowski equation (2) and the diffusion coefficients themselves are often calculated using hydrodynamic approximations where the diffusion coefficient is proportional to temperature and inversely proportional to viscosity. However, this hydrodynamic approximation is not valid over a large temperature range. An example concerns the hydroxyl radical [6]: at temperatures below the critical point, the diffusion coefficient of the radical is smaller than that of water even though the hydroxyl radical is smaller than the water molecule, but above the critical point, it exceeds that of the water molecule [6].

There are several examples of studies of elementary reactions in supercritical water (see as examples Refs. 8-10). In Ref. 9, Marin et al. studied reactions of two transient intermediates (hydrated electron and OH radical) relevant to radiation chemistry. Experimental values showed that the rate constants exhibit Arrhenius temperature dependence up to 200°C. After this point and up to close to the critical point, experimental rate constants exceed the extrapolated values. Around the critical temperature, the rate constant crosses over and dips below the extrapolated Arrhenius values. The cross-over and maximum around the critical point is similar to the findings of earlier work by Ghandi et al. [8]. The muonium kinetics studies by Ghandi et al. [8, 10] demonstrated that the rate constant goes through a maximum as the temperature increases, and that such behaviour may be a common feature for other reactions [5]. These results were explained using the cage effect: The reaction efficiency of bimolecular reactions in liquid solution depends on the frequency of collisions between the reaction partners while they are in close proximity (the “encounter pair”) due to the cage of surrounding solvent molecules. The main conclusion was that extrapolation of kinetic data from lower temperatures is not valid for modelling radiation chemistry in nuclear reactors [5].

3. Experimental

3.1 Mu and μSR

To probe kinetics in supercritical water we investigate the kinetics of muonium (Mu) reactions. Muonium (Mu = μ^+e^-), with a mass about one ninth that of its proton cousin, is simply the light isotope of the H-atom. Muons (μ^+, μ^-) occur naturally in cosmic-ray showers, but with minuscule intensity, and so of necessity are produced artificially at nuclear accelerators like TRIUMF in Vancouver, B.C. (Canada). Both the production ($\pi^+ \rightarrow \mu^+ + \nu_\mu$) and decay of positive muons ($\mu^+ \rightarrow e^+ + \nu_e + \nu_\mu$) are due to parity violation in the weak interaction, which forms the basis of the μSR technique [11]. The μ^+ is produced 100%

longitudinally spin polarized and its decay positron is subsequently emitted preferentially along the muon spin direction, providing a distinct signature of the time dependence of the muon polarization. Experiments can be carried out in either a transverse field (TF) or longitudinal field (LF) geometry. The experiments described here were all carried out in standard time-differential mode — the elapsed time is recorded between detection of an incoming μ^+ and its decay e^+. Simple plastic scintillators are sufficient to detect these charged particles.

The data acquisition system is logically defined to ensure only correlated muon-positron events are counted, for example by rejecting events for which more than one muon is present in a given time window. The μSR signature is generated by plotting a histogram of muon-positron events against the elapsed time (with ~1 ns bin widths). It has the general form

$$N(t) = N_0 e^{-t/\tau_\mu} \left[1 + A(t)\right] + b \tag{4}$$

where N_0 is an overall normalization factor which depends on the number of stopped muons and the detector geometry, b represents random accidental (background) events, $\tau_\mu = 2.197$ μs is the muon lifetime, and $A(t)$ represents the "asymmetry", which corresponds to the μSR signal of interest, and is similar to the free induction decay signal in conventional magnetic resonance.

The asymmetry parameter includes contributions from all muon environments, i.e. paramagnetic Mu and diamagnetic species such as MuH and MuOH. The components of the signal can have different precession frequencies (ω_i), phases (ϕ_i), amplitudes (A_i) and relaxation rates (λ_i), so in general

$$A(t) = \Sigma_i A_i \exp(-\lambda_i t) \cos(w_i t + \phi_i)\,. \tag{5}$$

In practice the precession frequencies of muons in diamagnetic environments are indistinguishable — they all precess at the same (muon Larmor) frequency. The Mu signal is characterized by much faster precession and it is detected at one or two frequencies, according to the strength of the applied magnetic field. At very low transverse field (TF) the signal has only two components:

$$S^{\mathrm{TF}}(t) = A_{\mathrm{Mu}} e^{-\lambda_{\mathrm{Mu}} t} \cos(w_{\mathrm{Mu}} t - \phi_{\mathrm{Mu}}) + A_{\mathrm{D}} \cos(w_{\mathrm{D}} t + \phi_{\mathrm{D}})\,. \tag{6}$$

The so-called "triplet" Mu precession frequency ω_{Mu} is 103 times faster than the diamagnetic muon precession, ω_{D}. This is evident in Figure 2, where the slow D precession is responsible for the curved background to the fast Mu oscillation. At intermediate fields ω_{Mu} splits into two.

The relaxation of the Mu signal (λ_{Mu}) is of particular importance since it represents chemical decay of muonium and/or spin relaxation caused by interaction of Mu with other paramagnetic atoms or molecules. The diamagnetic muon relaxation rate is invariably slow enough to be ignored in studies of Mu reactivity in liquids.

In the homogeneous kinetics regime of interest in this work the time dependence of the muon polarization in the Mu atom can be represented by the simple first-order decay expression:

$$[\mathrm{Mu}]_t = [\mathrm{Mu}]_0 e^{-\lambda_{\mathrm{Mu}} t} \quad (7)$$

where $\lambda_{\mathrm{Mu}} = k_{\mathrm{Mu}}[\mathrm{X}]$ is a pseudo first-order rate constant and k_{Mu} is the total rate constant for the reaction Mu + X with reactant "X". With only one Mu atom in the system at a time, the basis of the μSR technique is single-event counting, wherein Eqn. (7) invokes the "ergodic principle" in which a time-averaged ensemble is equivalent to a space-averaged one. The kinetics is thus always pseudo-first order and can be represented by the "concentration" of Mu atoms. Secondary reactions resulting from complex mechanisms will not affect the observed kinetics because the products of the primary Mu reaction are effectively invisible (spin dephased). Similarly, wall reactions can be ignored since at the densities of interest the diffusion time of Mu atoms to the walls of the target vessel is typically much longer than the muon lifetime. Thus the μSR technique is immune to many of the systematic errors and complications of H-atom kinetics studies, such as competition with other transients and radical scavengers.

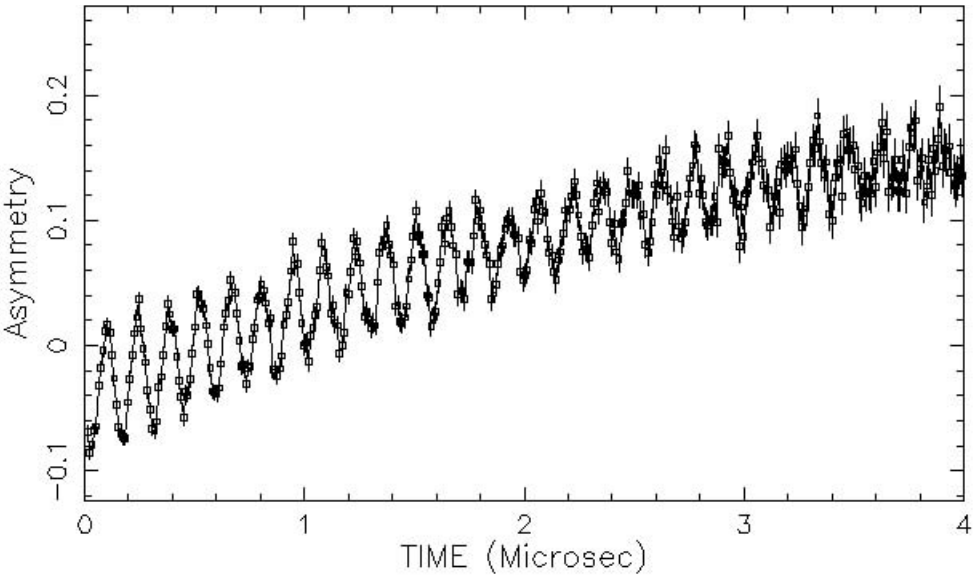

Figure 2 Muon asymmetry at 5 G transverse magnetic field for a solution of 1 mM LiOH in water at 420°C and 252 bar.

It should be noted that the total thermalization time of the muon is less than 1 ns, much smaller than typical reaction times, which are set by reactant concentrations to be on the order of 1 μs; therefore the Mu decay rate λ_{Mu} is a measure of thermal reaction rates.

In addition to chemical reaction the measured decay rate includes a component λ_b due to "background" relaxation, e.g. spin dephasing due to magnetic field inhomogeneity. There is also the possibility of spin exchange with paramagnetic impurities, typically dissolved oxygen. The total relaxation rate is expressed as

$$\lambda_{\mathrm{Mu}} = \lambda_{\mathrm{Ch}} + \kappa\lambda_{\mathrm{SE}} + \lambda_{\mathrm{b}} \quad (8)$$

where $\lambda_{Ch} = k_{Mu}[X]$ is due to chemical reaction of Mu with species X, and λ_{SE} is due to intermolecular spin exchange. The extent of the spin exchange contribution depends on the magnetic field, as expressed by the factor κ, which takes the value 1/2 in weak TF (< 10 G) and 3/4 for intermediate TF (~ 20 – 200 G) [12]. Thus, by varying the magnetic field a spin-exchange process can be distinguished from chemical reaction.

3.2 Experimental setup

Muon beams penetrate an entrance window and stop in a target cell of interest, which can be placed in a variety of μSR spectrometers with different magnetic fields and counter arrangements. Most measurements reported here were carried out in magnetic fields ~5 G, to ensure degenerate muonium precession (as described by Eqn. 6), and at intermediate fields (~20-30 G) to test for possible spin exchange from O_2 impurity as discussed above.

The target vessel used for measurements so far has a 2-3 mm thick titanium window to accommodate high pressures, up to 400 bar, necessitating the use of high energy "backward" muon beams. Thermostatically-controlled resistive heating coils are employed to heat the target vessel. An outer jacket is water-cooled to protect the plastic scintillator detectors outside the target assembly, and air is passed between the hot vessel and the outer jacket. This arrangement was used to achieve temperatures in the range of 25–450°C.

The experiments were carried out at the M9B muon channel of the TRIUMF cyclotron facility, using apparatus and procedures described previously [8, 10, 13, 14]. Samples (most recently, D_2O samples) were purged of oxygen by bubbling with nitrogen or argon prior to transfer to the evacuated pressure cell. Once in the pressure cell, the samples were heated and allowed to expand, or pressurized with a hand pump, to attain the desired thermodynamic conditions. Our pressure system includes an expansion vessel to accommodate changes in the density of the sample. By this means, we are able to control both pressure and temperature independently.

Typically, about 5 million correlated muon-positron events are accumulated in 1 hour (at ~ 150 μA proton beam intensity). An example of a muon asymmetry signal is presented in Figure 2. The oscillations due to Mu are clearly visible and it is straightforward to fit the histogram data with the appropriate theoretical expressions (Eqns. 4 and 6) to determine the Mu decay rate.

4. Previous studies of Mu kinetics in sub- and supercritical water

In our earlier studies [8, 10] we investigated answers to the following questions: How does the change in properties of water affect the rates of reactions in sub- and supercritical water? Are H atom reactions in supercritical water diffusion- or activation- controlled, or neither? Are cage effects important in near-critical conditions? We began our investigation by studying two reactions which have rate constants at or close to the diffusion limit at room temperature: (a) the electron spin exchange between Mu and Ni(II) ions; and (b) the addition of Mu to hydroquinone.

In the case of spin exchange, there is no atomic rearrangement when the two reactants encounter, and the exchange interaction is considered to require no activation energy, so in many respects this was expected to behave as the limiting case of a non-reactive diffusive encounter. It should be pointed out, however, that not all encounters result in a measurable spin flip [8]. For the case of Mu ($S = ½$) and Ni^{2+}_{aq} ($S = 1$) the electron spin exchange probability is $p_{spin} = 16/27$, but at the low transverse field used in this study the effective muon spin flip rate is only half this, i.e. 8/27 [8]. Figure 3 shows our experimental data. It is clear that the reaction is not diffusion-controlled, as rate constants decrease at higher temperatures.

Figure 3 Rate constants for Mu spin exchange with Ni^{2+} in water as a function of temperature at 240 bar [8].

Neither a diffusion model nor the Noyes equation could be fitted to the experimental data with reasonable parameters.

In the strong exchange limit, the probability of spin exchange depends only on p_{spin}. However, in the general case the probability depends on the encounter lifetime and the strength of the exchange interaction J [8].

$$k_{ex} = p_{spin} k_{diff} f_J; \quad f_J = J^2 \tau^2_{enc} / (1 + J^2 \tau^2_{enc}). \tag{9}$$

To estimate τ_{enc} we assumed that the concentration of encounter pairs is in equilibrium with the separated reactants, and that the equilibrium constant can be written as the ratio of rate constants for diffusion and separation of the reactants: $K_{enc} = k_{diff} / \tau^{-1}_{enc}$. Using a statistical argument [8] K_{enc} can be roughly estimated by considering the probability of finding one reactant as the next nearest neighbour to the other. Taken a coordination number of 8, we found $K_{enc} = 8/[H_2O]$, so that

$$\tau_{enc} = 8 k^{-1}_{diff} \big/ \left[H_2O \right] \tag{10}$$

Figure 4 compares experimental values of f_J with predictions. The data corresponds to the Mu + Ni(II) rate constants divided by ($p_{spin}k_{diff}$). The curve was computed with encounter times calculated from Eqn. (10) and one adjustable parameter: $J = 1.4 \times 10^{12}$ rad s^{-1}.

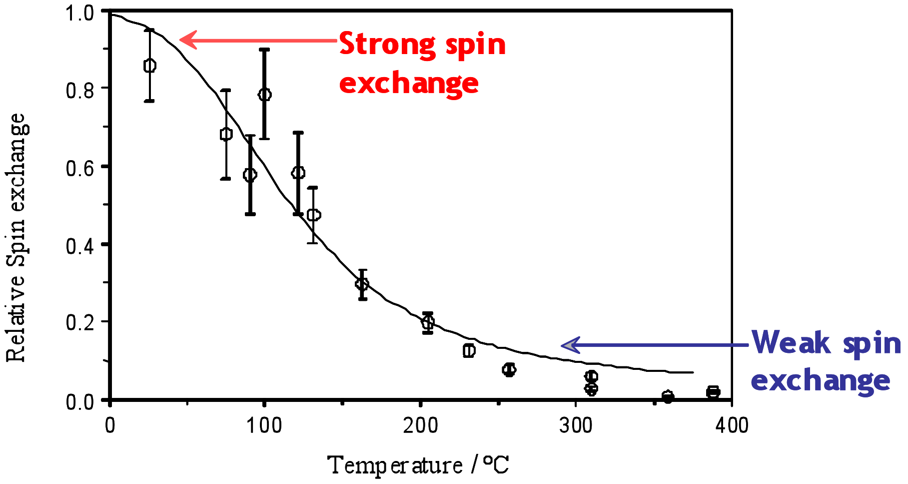

Figure 4 Spin exchange probability between Mu and Ni^{2+} as a function of temperature at 240 bar.

The decrease of encounter time at higher temperatures causes an inefficient spin exchange; hence the rate constant decreases at high temperatures. Does a decrease in the encounter time also result in a drop-off in efficiency of chemical reactions? We investigated this question in our study of the Mu reaction with hydroquinone [8], and confirmed the effect with several other reactions [9], as indicated by the data shown in Figure 5.

We described this decrease in efficiency of chemical reactions at higher temperatures with the drop in number of collisions per each encounter by introducing an efficiency factor *f*. In terms of the cage effect, *f* depends on the number of collisions that occur between the reactants over the lifetime of the encounter pair. This is evident if the situation is viewed as a simple competition between the reaction and escape of the reactants from the cage:

$$f = p\tau_{\mathrm{coll}}^{-1} \big/ (\tau_{\mathrm{enc}}^{-1} + p\tau_{\mathrm{coll}}^{-1}) = pq \big/ (1 + pq) \qquad (11)$$

where $q = \tau_{\mathrm{enc}} / \tau_{\mathrm{coll}}$ gives the number of collisions per encounter (Figure 6). The key factor in the fall-off with temperature seems to be the drop in the number of collisions between a pair of reactants over the duration of their encounter.

5. New experimental data

In view of our previous findings, we decided to study a reaction where this cage effect would not be important. A reaction between a reactant and the solvent molecules would not follow such a cage effect. Therefore, we studied reaction of Mu and D_2O at higher temperatures. The reaction is too slow to observe significant relaxation at lower temperatures. The reaction is also important in view of the significance of reaction $H + H_2O \rightarrow H_2 + OH$ in radiolysis of water and as a potential source of H_2 formation in the coolant of an SCWR.

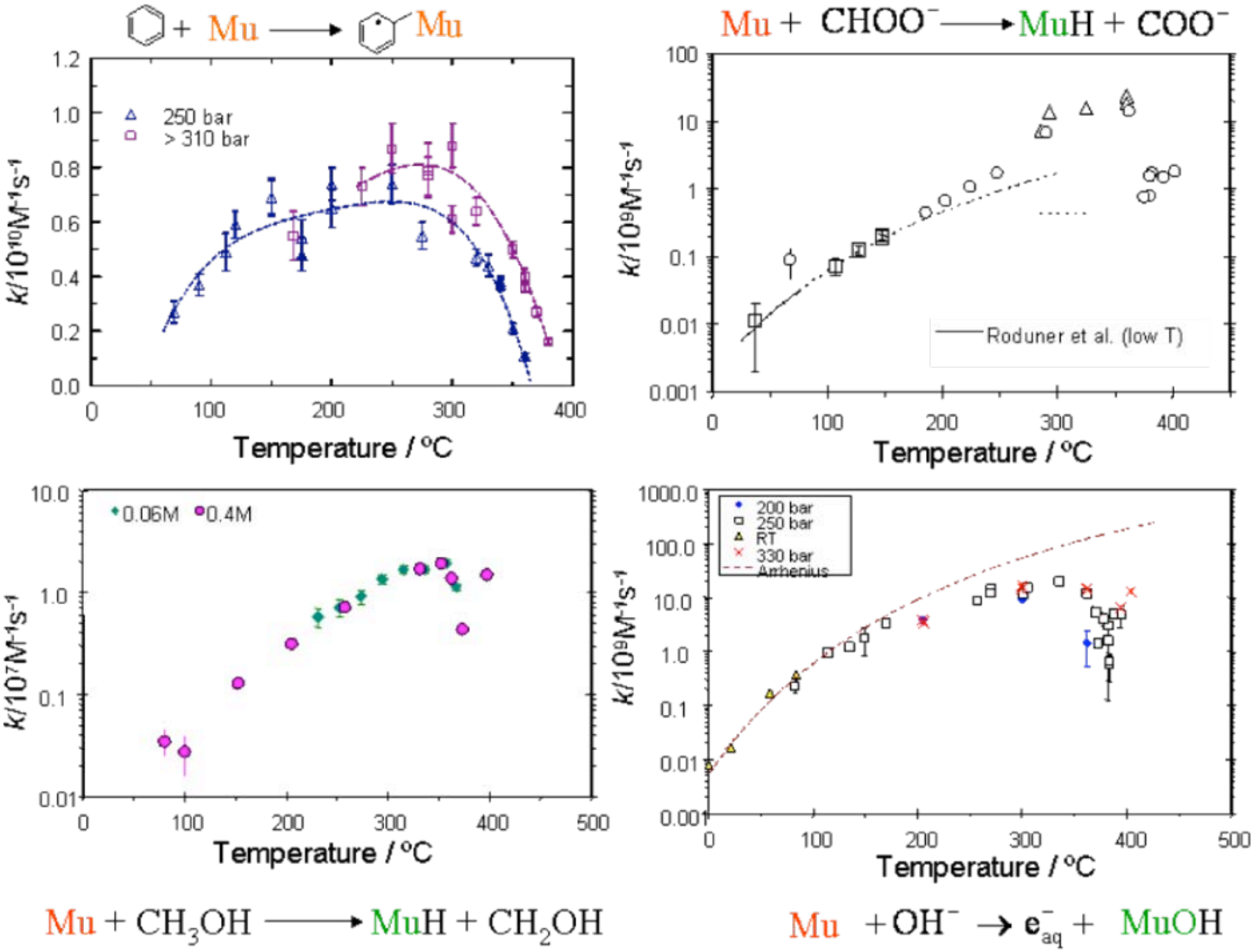

Figure 5 Rate constants for different reactions as a function of temperature under isobaric conditions.

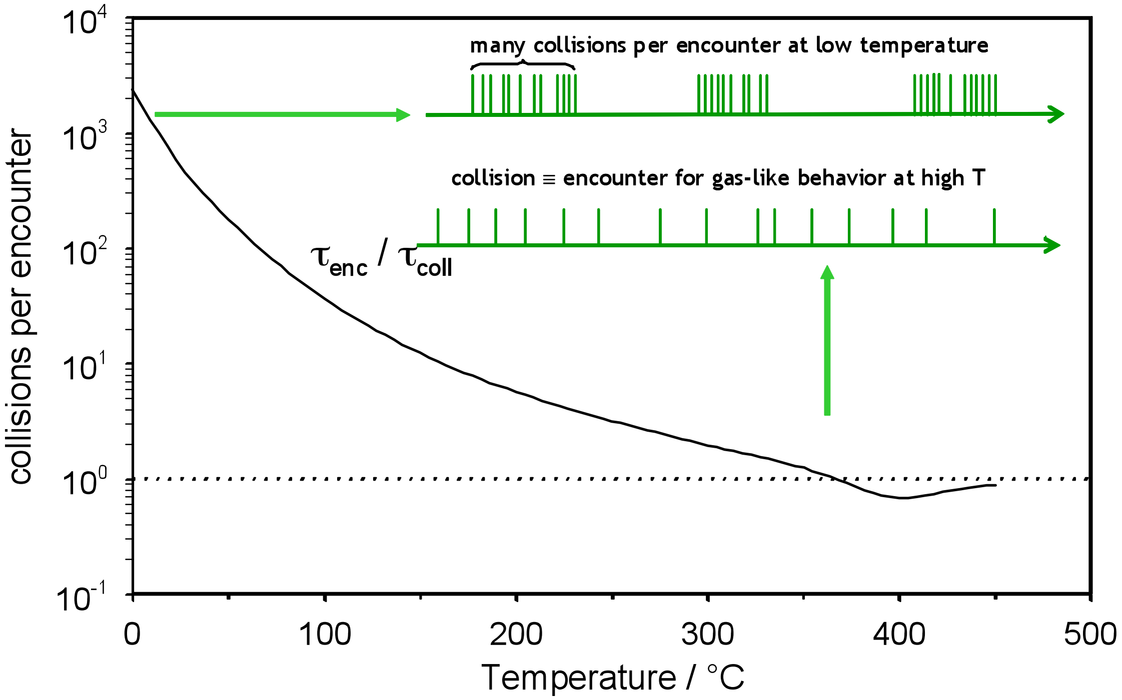

Figure 6 Number of collisions per encounter as a function of temperature at 240 bar.

The bimolecular rate constant is calculated from the muonium decay rate:

$$k_{\mathrm{Mu}} = \frac{(\lambda_{\exp} - \lambda_0)}{[\mathrm{X}]_0} \cdot \frac{\rho_0}{\rho(T,P)} \tag{12}$$

where $[X]_0$ is the D_2O concentration under standard conditions, ρ_0 is the density under standard conditions, λ_0 is the background relaxation rate and ρ is the density, which varies with temperature and pressure.

Muonium decay rates and the rate constants calculated from Eqn. (12) are listed in Table 1. Figure 7 presents the Arrhenius plot of our data at constant pressure while Figure 8 shows the pressure dependence of rate constants at constant temperature.

The reaction of the hydrogen atom with water may be important in high temperature radiolysis of water and therefore a knowledge of its rate constant is required [15]. It has been pointed out that the contribution of this reaction to the spur chemistry in high temperature pressurized water may be responsible for the unexplained increase in the molecular hydrogen yield [16]. Using diffusion-kinetic modelling Swiatla-Wojcik and Buxton deduced that a rate constant of 3.2×10^4 $M^{-1}s^{-1}$ for the reaction $H + H_2O \rightarrow H_2 + OH$ is needed to explain the temperature effect on the radiation chemical yield of H_2.

Table 1 Muonium decay rates in D_2O at various temperatures (T) and pressures (P), and the rate constants calculated from Eqn. (12).

$[D_2O]$ /M	T /°C	P /bar	ρ /g·cm^{-3}	λ_{exp} /10^6 s^{-1}	λ_0 /10^6 s^{-1}	k_{Mu} /10^3 M^{-1}s^{-1}
26.9	385.0	298.0	0.539	0.37 ± 0.03	0.125	9.0 ± 1.7
23.3	392.5	299.0	0.466	0.36 ± 0.02	0.125	10.1 ± 1.8
19.0	400.0	300.0	0.380	0.34 ± 0.01	0.125	11.1 ± 2.1
27.4	385.0	304.0	0.549	0.35 ± 0.02	0.125	8.3 ± 1.6
14.5	385.0	226.0	0.290	0.20 ± 0.02	0.125	5.4 ± 2.8
12.9	385.0	245.0	0.257	0.21 ± 0.01	0.125	6.8 ± 3.0
15.0	385.0	250.0	0.301	0.25 ± 0.01	0.125	8.5 ± 2.6
20.0	385.0	260.0	0.401	0.34 ± 0.02	0.125	10.9 ± 2.0
29.9	385.0	349.2	0.598	0.62 ± 0.04	0.125	16.6 ± 1.9
27.1	385.0	300.0	0.543	0.56 ± 0.04	0.125	15.9 ± 2.0

In more recent work Bartels has used another approach to estimate the rate constant for the above reaction [17]. He estimated a rate constant of ~ 2.2×10^3 M^{-1}s^{-1} for the reaction at 300°C. Considering the importance of H_2 concentrations in the coolant to reduce the dissolved oxygen concentration and minimize the susceptibility of intergranular stress corrosion cracking, an experimental measurement of this rate constant and the rate constants of its isotopic analogues is essential. To that end, our investigations may shed some light on the controversies regarding the reaction of the H atom with water [15-17].

Our rate constants are similar in order of magnitude to the above estimates [16, 17] and lie between them (although closer to Bartels' value). Our measured activation energy (15 ± 3 kcal mol^{-1}) is similar to the estimate in Ref. 16 (between 14 and 19 kcal mol^{-1}); however, the zero-point vibrational effects need to be included for a more accurate comparison and to use our data to check the validity of the above estimations. Also, the relaxation could be partially due to reaction with OD^-, formed by ionic dissociation of D_2O. Its concentration varies according to the temperature and density dependence of the pK_W. The maximum concentration of OD^- is at temperatures between 250°C and 325°C.

Due to the importance of this reaction we are currently extending our investigations to a wide range of temperatures and pressures for both H_2O and D_2O. Also, we are investigating the Mu reaction with OH^- and OD^-. When we conclude these studies we should be able to distinguish between the contributions of the Mu reactions with H_2O itself and with OH^- from ionic dissociation of H_2O. We are also carrying out modelling studies of these reactions, by ab inito quantum calculations using continum and cluster simulations.

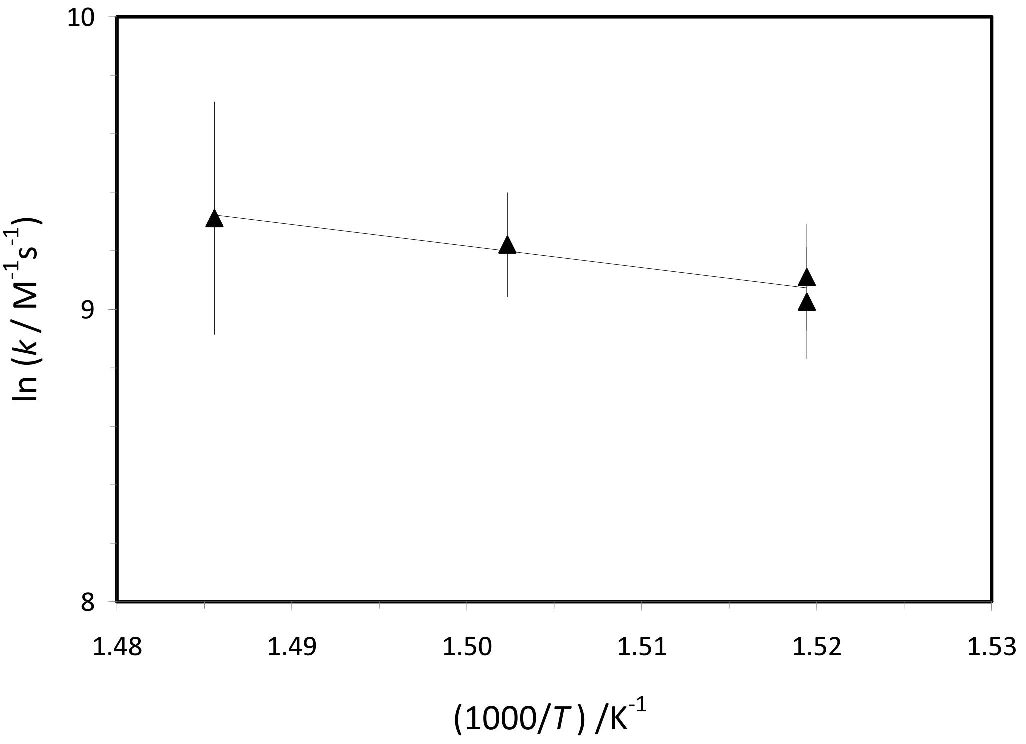

Figure 7 Rate constants for the reaction of Mu with D_2O at ~300 bar.

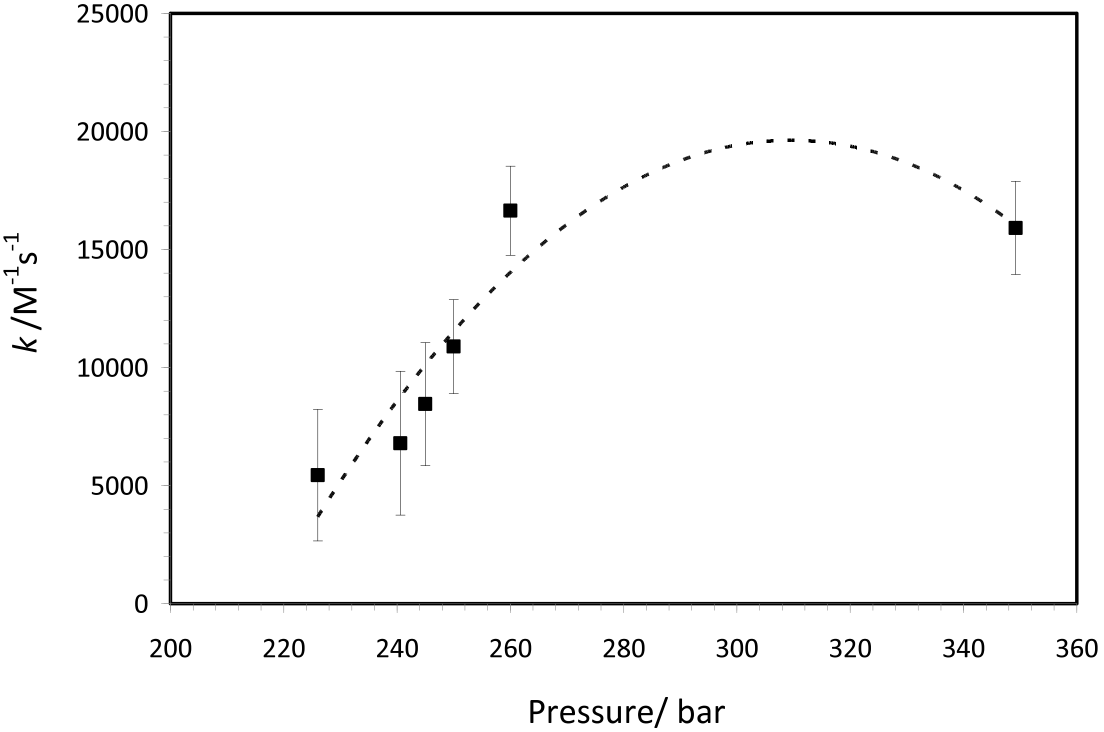

Figure 8 Rate constants for the reaction of Mu with D_2O at 385°C.
The lines through the data are to guide the eyes only.

6. Conclusion

The rate constants of bimolecular reactions in near critical water change with temperature in a non-Arrhenius fashion. The key factor is the number of collisions per encounter of the reaction partners. This consideration is unimportant for reaction of a solute with the solvent itself, as demonstrated by our kinetics study of the reaction of Mu with D_2O. There is some controversy regarding the importance of the reaction $H + H_2O \rightarrow H_2 + OH$ to the radiolysis of water, and our preliminary results suggest that it may have a significant rate under near critical conditions. If so, its contribution to the yield of H_2 could be important to the development of chemistry control strategies for a Gen IV SCWR.

7. Acknowledgments

We thank Dr. Syd Kreitzman and the staff of the TRIUMF μSR facility for their technical support. Financial support from the Natural Sciences and Engineering Research Council of Canada, National Research Council and Atomic Energy of Canada Limited is also greatly appreciated. We thank Ms. Pooja Vyas and Mr. Brendan Baartman for their assistance during beam time.

8. References

[1] M. Wakita and K. Kitano, "Decomposition of organic wastes by down flow supercritical water oxidation system", *Environmental Conservation Engineering*, 32, 2003, 17.

[2] J. Yoo, Y. Ishiwatari, Y. Oka, J. Yang and J. Liu, "Subchannel analysis of supercritical light water-cooled fast reactor assembly", *Nuclear Engineering and Design*, 237, 2007, 1096.

[3] M Siskin and A.R. Katritzky, "Reactivity of organic compounds in superheated water: General background", *Chem. Rev.*, 101, 2002, 825; A.R. Katritzky, D.A. Nichols, M. Siskin, R. Murugan, and M. Balasubramanian, "Reactions in high-temperature aqueous media", *Chem. Rev.*, 101, 2002, 837.

[4] A. J. Elliot, D.R. McCracken, G.V. Buxton and N.D. Wood, "Estimation of rate constants for near-diffusion-controlled reactions in water at high temperatures" *J. Chem. Soc. Faraday Trans*., 86, 1990, 1539.

[5] K. Ghandi and P. Percival, "Prediction of rate constants for reactions of the hydroxyl radical at high temperatures and pressures", *J. Phys. Chem. A*, 107, 2003, 3005.

[6] I.M. Svishchev and A. Plugatyr, "Supercritical water oxidation of o-dichlorobenzene: degradation studies and simulation insights", *J. of Supercritical Fluids*, 37, 2006, 94.

[7] J.T. Henrikson and P.E. Savage, "Potential explanations for the inhibition and acceleration of phenol SCWO by water", *Ind. Eng. Chem. Res*., 43, 2004, 4841; J.T. Henrikson, R.C. Grice and P.E. Savage, "Effect of water density on methanol oxidation kinetics in supercritical water", *J. Phys. Chem. A*., 110, 2006, 3627.

[8] K. Ghandi, J. Brodovitch, B. Addison-Jones, I. McKenzie, P.W. Percival and J. Schüth, “Near diffusion-controlled reactions of muonium in supercritical water”, *Phys. Chem. Chem. Phys*., 4, 2002, 586.

[9] T.W. Marin, J.A. Cline, K. Takahashi, D.M. Bartels and C.D. Charles, “Pulse radiolysis of supercritical water: reaction of nitrobenzene with hydrated electrons and hydroxyl radicals”, *J. Phys. Chem. A*, 106, 2002, 12270.

[10] K. Ghandi, B. Addison-Jones, J.-C. Brodovitch, S. Kecman, I. McKenzie and P.W. Percival. “Muonium kinetics in sub- and supercritical water”, *Physica B*, 326, 2003, 76

[11] E. Roduner, “Polarized positive muons probing free radicals: a variant of magnetic resonance”, *Chem. Soc. Rev*., 22, 1993, 337.

[12] M. Senba, “Anisotropic muonium atoms: Energy levels and electron spin exchange”, *Phys. Rev. A*, 62, 2000, 042505.

[13] P.W. Percival, J.-C. Brodovitch, K. Ghandi, B. Addison-Jones, J. Schüth and D.M. Bartels, “Muonium formation in sub-and supercritical water”, *Phys. Chem. Chem. Phys*., 1, 1999, 4999.

[14] J.-C. Brodovitch, “Apparatus for μSR and μLCR experiments on fluids at high pressure and temperature”, *Physica B*, 374-375, 2006, 314.

[15] H.E. Sims,”Yields of radiolysis products from gamma irradiated supercritical water a reanalysis data by W.G. Burns and W.R. Marsh”, *Radiat. Phys. Chem*., 75, 2006, 1047.

[16] D. Swiatla-Wojcik and G.V. Buxton, “On the possible role of the reaction $H+H_2O \rightarrow H_2+OH$ in the radiolysis of water at high temperatures”, *Radiat. Phys. Chem*., 74, 2005, 210.

[17] D.M. Bartels, “Comment on the possible role of the reaction $H+H_2O \rightarrow H_2+OH$ in the radiolysis of water at high temperatures”, *Radiat. Phys. Chem*., 78, 2009, 191.